In-situ utilization of iron flocs after Fe^{3+} coagulation enhances H_2O_2 chemical cleaning to eliminate virus and mitigate ultrafiltration membrane fouling

*Zixiao Ren [a], Huicong Shi [a], Jie Zeng [a], Xu He [a], Guibai Li [a], Huu Hao Ngo [b], Jun Ma [a], Chuyang Y. Tang [c], An Ding [a]**

a. *State Key Laboratory of Urban Water Resource and Environment, School of Environment, Harbin Institute of Technology, Harbin, 150090, P. R. China*

b. Faculty of Engineering, University of Technology Sydney, P.O. Box 123, Broadway, Sydney, NSW 2007, Australia

c. Department of Civil Engineering, The University of Hong Kong, Pokfulam, Hong Kong 999077, China

*Corresponding author.

E-mail address: dinganhit@163.com (An Ding)

Graphical abstract

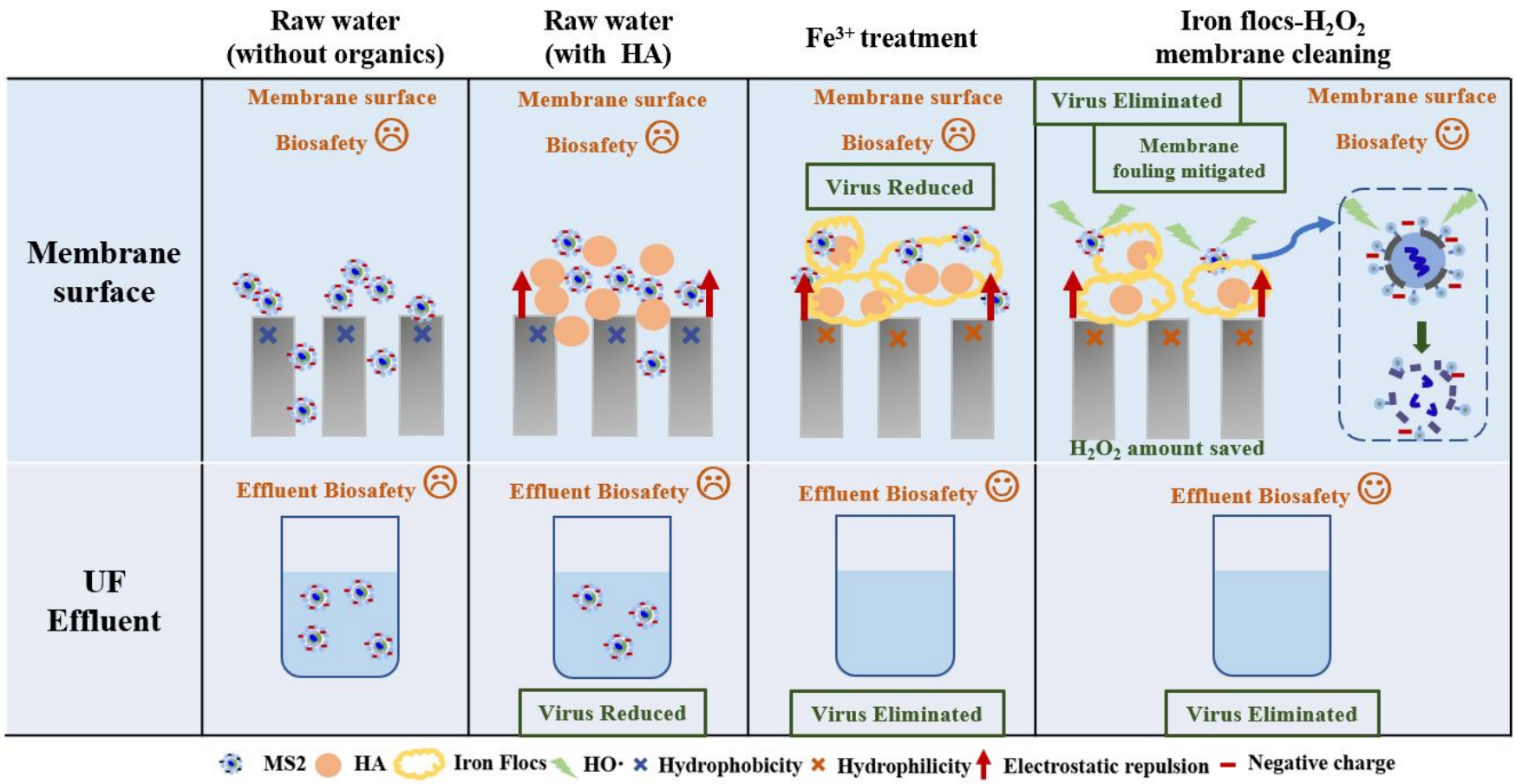

Abstract

Viruses found in effluent and on membrane surface during ultrafiltration (UF) processes will introduce hidden biosecurity dangers to drinking water. Fe^{3+} coagulation and H_2O_2 were combined to create an in-situ membrane cleaning method in this study, and MS2 bacteriophage was used as a model to investigate virus removal by UF when humic acid (HA) was present in raw water. The results showed that 0.50 log PFU/mL MS2 was removed by UF when HA concentration was 6 mg/L based on size exclusion, hydrophobicity, and electrostatic repulsion. Meanwhile, HA inhibiting the adsorption of MS2 to the membrane surface, which slightly reduced MS2 accumulation on membrane surface. A 0.08 mmol/L Fe^{3+} pretreatment eliminated MS2 in the effluent by the adsorption and size exclusion of iron flocs. Furthermore, the number of MS2 retained on the membrane surface dropped from 5.84 log PFU/cm^2 to 3.84 log PFU/cm^2 through electrostatic repulsion. MS2 on the membrane surface was effectively inactivated with viral protein capsid destroyed by in-situ cleaning of iron flocs-H_2O_2 through HO· oxidation. The mitigation efficiency of membrane fouling was greatly improved with a flux recovery of 97.8%. Moreover, the amount of H_2O_2 was reduced (3%) compared to no Fe^{3+} pretreatment (12%), which could greatly save costs. This study provides a potentially useful and economical enhanced membrane cleaning method for virus-containing water treatment by UF, which could not only eliminate viruses and mitigate membrane fouling in UF system but also reduce the use of membrane cleaning agents to save costs.

Keywords: Ultrafiltration; NOM; virus removal; iron flocs-H_2O_2; in-situ cleaning

1. Introduction

Ultrafiltration (UF) is a promising physico-chemical process to remove virus in drinking water, showing the advantages of high efficiency and low risks of virus mutation, drug resistance, etc. [1-5]. However, some viruses with small diameters, such as adenovirus, rotavirus, norovirus, bacteriophage, etc., can still pass through the pores of UF membranes [6-9]. Ozone, ultraviolet, and chlorine disinfection are traditional methods to inactivate pathogens in drinking water plants operation [10-13]. These methods, however, may not be effective in the removal of some strongly resistant viruses [7]. For this reason, how to improve the virus retention efficiency by UF is an urgent issue that needs to be solved.

Viruses can be removed during membrane treatment by various mechanisms, such as electrostatic repulsion, size exclusion, hydrophobic interaction and adsorption [14-16]. Natural organic matter (NOM) in feedwater can promote virus retention efficiency through multiple mechanisms [17-20]. The accumulation of organics on the membrane surface will increase virus interception and improve the contribution of size exclusion on virus removal. ElHadidy et al reported that virus removal was improved by humic substances adhering to the membrane surface and the increase of negative charge and hydrophobicity [19]. However, NOM will aggravate membrane fouling and cause increased energy consumption [20-22]. Therefore, it is imperative to devise a strategy that can not only reduce viruses in the effluent but also mitigate membrane fouling.

Coagulation pre-treatment can be an effective solution to simultaneously reduce membrane fouling and enhance virus removal [23-26]. Kreißel et al. reported that low dosages

of polyaluminum chloride (PACl) coagulation treatment could inactivate MS2 and Qβ bacteriophages [27]. Zhu et al. demonstrated over 4-log MS2 removal by iron coagulation enhanced microfiltration, which was significantly higher than microfiltration alone [28]. The virus removal will be improved by adsorbing onto iron flocs. In addition, the band gap of iron oxides may play a role in microorganism inactivation [29]. However, NOM in raw water may consume the dosage of coagulant and reduce the virus removal rate, Fe^{2+} oxidation, precipitation, and virus destabilization will be inhibited. [30]. Even if viruses are completely removed from the effluent by pretreatment, viruses retained on the membrane surface can still pose a serious biological risk during the disposal process of the discarded membrane or require large amounts of additional disinfectant consumption.

Chemical cleaning has high efficiency in mitigating membrane fouling and removing foulants [31-34]. Irreversible fouling resistance is an important contributor to virus interception [35, 36] and can only be effectively removed by chemical cleaning. Hydrogen peroxide (H_2O_2) is also a commonly used membrane-cleaning agent as well as disinfection, can destroy the pathogenic microbial structure [37, 38]. Li et al. recently proposed a FeOx+MnOx+H_2O_2 membrane cleaning strategy, and it effectively improved membrane flux and reduced irreversible fouling resistance [39]. Hydroxyl radicals (HO·) generated by catalyzing H_2O_2 can effectively inactivate MS2 by denaturing protein capsids. Mamane et al. reported that 2.5-logs inactivation of MS2 was obtained after the treatment of UV/H_2O_2 [40]. H_2O_2 chemical cleaning coupled with iron flocs after coagulation may play a more efficient role in disinfection and membrane fouling mitigation.

Therefore, this study aims to create an in-situ cleaning method by utilizing the iron flocs generated after coagulation combined with H_2O_2 chemical cleaning to guarantee drinking water biosecurity and alleviate membrane fouling. MS2 bacteriophage with a similar shape and size to polio and hepatitis viruses [41] was used as a virual model to study the following: (1) the influence and mechanism of Fe^{3+} coagulation on MS2 removal in effluent and on the UF membrane surface when humic acid (HA) presented in feedwater; (2) performance of iron flocs-H_2O_2 in-situ cleaning on the further removal of MS2 remaining on the membrane surface and membrane fouling mitigation; and (3) the mechanism contribution on MS2 removal during different treatment stages.

2. Materials and methods

2.1 MS2 stock preparation

The stock of MS2 bacteriophage was prepared with the method employed by Anderson et al. [42]. Liquid LB-medium was used to cultivate E-coli (ATCC 15597) at 37℃ with a shaking speed of 150 rpm. MS2 stock (ATCC 15597-B1) was then put into E-coli stock (with a concentration of 3×10^8 cells/mL^{-1}) at the ratio of 1:1 and cultivated in conditions of 37℃ and 150 rpm. The MS2 suspension was centrifuged at 10000 g for 20 min. E-coli cells and cell debris in the supernatant were removed by a 0.22 μm filter (Jinteng, Tianjin, China). The MS2 stock was obtained with a concentration of 2×10^9 PFU/mL^{-1}.

2.2 Pre-coagulation with $FeCl_3$

The feed water consisted of MS2 bacteriophage and HA with the dosage of 0.5, 1, 2,

3, 6 mg/L, in which the concentration of MS2 was 1.22×10^6 PFU/mL. $FeCl_3$ (Basifu, Tianjin, China) was selected as the coagulant. The employed concentrations of $FeCl_3$ were 0.01, 0.02, 0.04, 0.08 mmol/L, respectively. The stirring conditions of coagulation were 700 r/min for 2 min and then 150 r/min for 15 min. The water samples after coagulation were used for the follow-up UF process.

2.3 Membrane filtration

A polyethersulfone UF membrane with a molecular weight cut-off (MWCO) of 150 kDa was employed (UP150, Microdyn-Nadir, Germany). The UF system shown in **Fig. S1**, which consisted of a UF cell to operate filtration (UFSC40001, Millipore Amicon, US), a nitrogen gas cylinder (provide a constant pressure of 0.04 MPa), and an electronic balance (BSA2202S, Sartorius, Germany) connected to a computer (automatically recorded weight data every 4 s). Preservatives on the membrane surface were removed by immersing virgin membranes in 50% ethanol solution for 15 min. During the UF process, the membranes with a surface area of 39 cm^2 were put with their smooth side up at the bottom of the UF cell. The pure water flux was calculated by filtering Milli-Q water before and after the UF process. After 450 mL water samples were filtered, a brush was used to clean and collect foulants on the fouled membrane surface. 0.1 mmol/L $NaHCO_3$ (Tianda, Tianjin, China) solution was used to rinse the membrane surface to collect the foulants that were brushed off. The flushing fluid was used to measure the MS2 numbers that resided on the membrane surface.

2.4 Chemical cleaning for fouled membrane

The fouled membranes were immersed in 100 mL H_2O_2 (Beilian, Tianjin, China) solution with concentrations of 1%, 3%, 6%, 9%, and 12% for 5 min to conduct chemical cleaning procedure. After that, the membranes were taken out and washed with Milli-Q water to remove residual H_2O_2. Subsequently, the membranes after chemical cleaning were cleaned with a brush and collected flushing fluid to measure the MS2 numbers that resided on the membrane surface.

2.5 Analytical methods

2.5.1 Bacteriophage assays

The standard plaque-forming unit (PFU) assay was employed to determine the concentration of MS2 in the effluent and the amount of MS2 on the membrane surface. Briefly, 0.1 mL water sample and 0.1 mL E-coli solution at the logarithmic phase were mixed with 3 mL semi-solid LB-medium. The mixture was poured onto the solid LB-medium plates and allowed to solidify. The MS2 plagues were counted after the plates were incubated at 37℃ overnight. The concentration and numbers of MS2 were calculated by Eq. (1, 2) as written here:

$$\log_c = \log\left(\frac{N_t}{V}\right) \quad (1)$$

$$\log_n = \log\left(\frac{N_t}{S}\right) \quad (2)$$

where: $\log_c$ represents the concentration of MS2 in the effluent (PFU/mL); $\log_n$ denotes the amount of MS2 remaining on the membrane surface (PFU/cm^2); N_t is the total number of residual MS2 after filtration; V stands for the volume of feed water (450 mL); S

is the area of UF membrane (39 cm^2). The morphology and adsorption of MS2 were observed by Transmission Electron Microscopy (TEM; JEM1400010101).

2.5.2 Water quality analysis

The UV_{254} values of HA were measured by a UV-Spectrophotometer (UV759CRT, Youke, China). A laser particle size analyzer (S90, Malvern Panalytical, UK) was used to determine the particle size distribution of water samples. A Zetasizer instrument (S90, Malvern Panalytical, UK) was employed to analyze the Zeta potential of water samples.

2.5.3 Analysis of membrane fouling

The specific flux (J/J_0) showed the trend of flux decline during UF process. **Text S1** in **Supplementary Information** showed the method for calculating membrane fouling resistances, which consist of hydraulic reversible (*Rr*) and irreversible fouling resistances (*Rir*). The significant difference between two data groups was analyzed by the T-test. A pore blockage-cake filtration model [5] was applied to evaluate membrane fouling mechanism.

2.5.4 Membrane surface characterization

Membrane surface zeta potential was observed by SurPASS 3 (Anton Paar, Austria). A contact angle measuring device (SL150, Kino, USA) was used to determine the membrane surface hydrophobicities. The contact angles were measured with three different types of liquid: Milli-Q water, diiodomethane and glycerol. XDLVO theories were used to analyze the interactions between virus and membrane surfaces. The calculation method employed for the XDLVO theories was based on the study by Gentile et al. [43]. Fourier

transform infrared spectroscopy (FTIR) was measured to explore the functional group changes of membrane surface (Spectrum One PerkinElmer, USA). The transformation of MS2 capsid protein secondary structures was analyzed by the software of Peakfit 4.12 (Software Inc., USA).

3. Results and discussion

3.1 Contribution of HA in feedwater to MS2 removal

3.1.1 MS2 removal

The concentration of MS2 in effluent and the amount of MS2 that remained on the membrane surface are shown in **Fig. 1 (a)**. 3.98 log PFU/mL MS2 passed UF membrane while 6.08 log PFU/cm^2 MS2 was retained by the membrane surface when the influent contained no HA. The large amount of MS2 residing on the membrane surface would mean that a dangerous biosafety risk may emerge. The retention of MS2 by the membrane surface fell slightly with the increase of HA concentration, the remaining number dropped to 5.84 PFU/cm^2 with only 4.0% removal rate at 6 mg/L HA. This phenomenon was attributed to HA inhibiting the adsorption of viruses on membranes, reducing their ability to retain viruses during UF [44-46]. The increase in HA dosage had a more significant effect on MS2 removal in the effluent, to the extent that MS2 concentration decreased to 3.48 log PFU/mL and the removal rate reached 12.6%.

Fig. 1 (a) MS2 in effluent and on the membrane surface under different HA dosages after UF, (b) membrane flux after MS2 and HA fouling; (c) membrane fouling resistance after MS2 and HA fouling; (d) particle size of MS2 and HA+MS2.

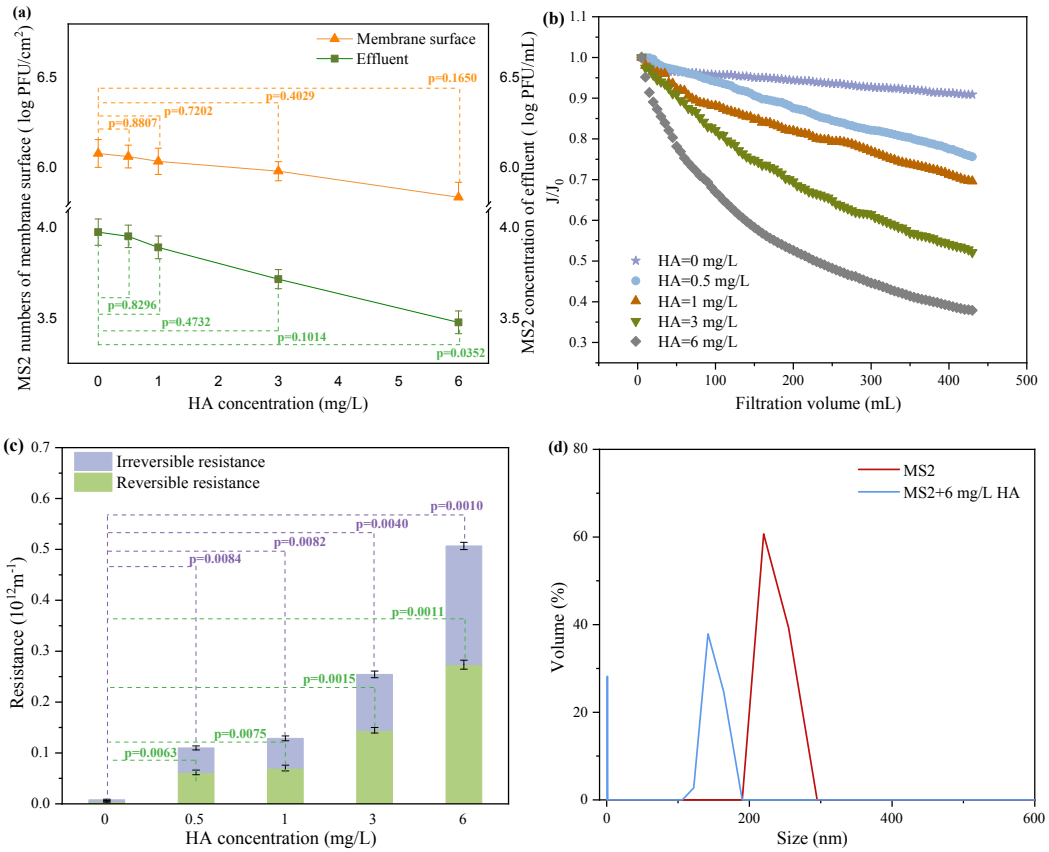

191

192

193 **3.1.2 HA and MS2 caused severe membrane fouling**

194 Individual MS2 caused slight membrane fouling, the final flux only declined to 0.91

195 and the dominant fouling mechanism was intermediate blocking (**Table 1**). HA exacerbated

196 membrane flux decline and 6 mg/L HA caused the final flux declined to 0.38 (**Fig. 1 (b)**).

197 The dominant fouling mechanisms turned into complete blocking and cake filtration with

198 the HA accumulation in the membrane pores and on the membrane surface (**Table 1**).

199 Previous studies have proved that irreversible fouling resistance and cake layer will help to

200 enhance the removal rate of virus [46, 47].

201 **Fig. 1 (c)** indicates that the membrane fouling resistance caused by MS2 and HA was

202 dominated by reversible resistance. The reversible & irreversible resistances caused by

203 MS2 were similar, both measured at 0.04×10^{11} m^{-1}. HA greatly increased the fouling

resistance and reversible reached 2.74×10^{11} m^{-1}, as well as irreversible fouling resistance, rose up to 2.33×10^{11} m^{-1} when HA dosage was 6 mg/L. Irreversible fouling has achieved a higher proportion in total fouling resistance that was beneficial to the retention of MS2. The greatly improved membrane fouling resistance ($p<0.05$) blocked MS2 from passing the UF membrane by size exclusion, which was one of the important factors affecting virus removal [19]. But the increased irreversible fouling exacerbates membrane fouling and also improved the difficulty of membrane cleaning.

Table 1 Membrane fouling model fitting under different conditions.

R^2	Intermediate Blocking	Standard Blocking	Complete Blocking	Cake Filtration
MS2	**0.9881**	0.9714	0.9645	0.9680
0.5 mg/L HA +MS2	0.9760	**0.9894**	0.9796	0.9799
1 mg/L HA +MS2	0.9651	**0.9998**	0.9762	0.9799
3 mg/L HA +MS2	0.9618	0.9754	**0.9868**	**0.9982**
6 mg/L HA +MS2	0.9032	0.9070	**0.9801**	**0.9976**
0.01 mmol/L Fe^{3+} pretreatment	0.9772	**0.9847**	**0.9901**	**0.9962**
0.02 mmol/L Fe^{3+} pretreatment	0.9728	**0.9814**	0.9730	**0.9810**
0.04 mmol/L Fe^{3+} pretreatment	0.9784	0.9614	**0.9981**	**0.9976**
0.08 mmol/L Fe^{3+} pretreatment	0.8714	0.9545	0.9753	**0.9974**

(Bold items represent R^2 values > 0.98)

3.1.3 The mechanism of how HA improves virus removal

The above discussion demonstrated that size exclusion due to aggravated membrane fouling was one of the main mechanisms for removing a virus. MS2 slightly increased the membrane surface electronegativity from -15.25 mV to -15.31 mV. HA with a negative charge further improved the electronegativity (**Fig. 2 (a)**) and enhanced the electrostatic repulsion both in the solution and between MS2 and the membrane surface (**Fig. 2 (b) (c)**), which contributed to MS2 removal. Changes in membrane surface hydrophilicity and

hydrophobicity have certain effects on virus removal. Hydrophobic MS2 enhanced membrane surface hydrophobicity after filtration (**Table 2**). The membrane surface hydrophobicity was further enhanced after 6 mg/L HA and MS2 passed the UF membrane, which was beneficial for removing the virus [15, 48].

Overall, the promotion of virus removal in the effluent and on the membrane surface was the outcome of the combined enhancement of membrane surface hydrophobicity, electrostatic, and repulsion size exclusion after HA fouling.

Fig. 2 (a) Zeta potential of the membrane surface; (b) interaction force in solution; and (c) interaction force between the membrane surface and foulants.

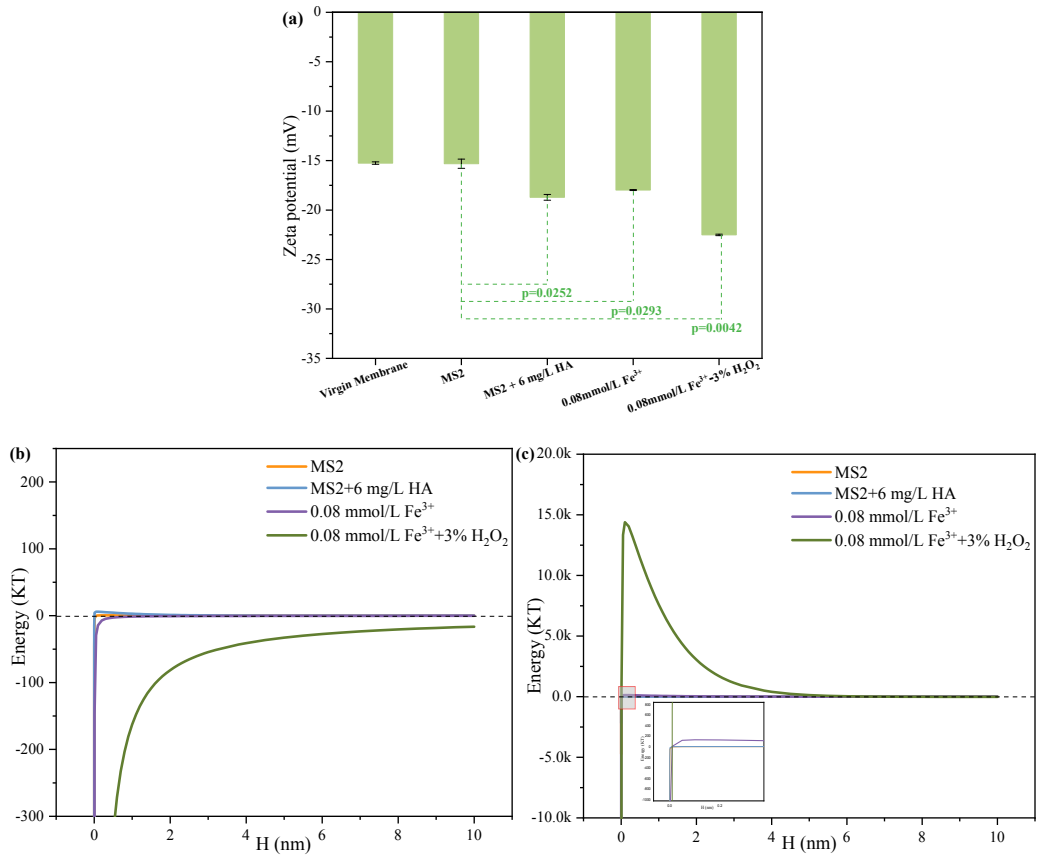

Table 2 Effect of different treatments on the contact angle of the membrane surface.

Group	Contact Angle of Water (°)
Virgin membrane	51.61

MS2	52.01
MS2+HA	56.92
0.08mmol/L Fe^{3+} treatment	47.19
0.08mmol/L Fe^{3+}-3% H_2O_2 Cleaning	45.14

3.2 Influence and mechanism of MS2 inactivation in effluent and on membrane surface by Fe^{3+}

3.2.1 Removal of MS2

The removal of MS2 in the effluent and on the membrane surface after Fe^{3+} coagulation was shown in **Fig. 3 (a)**. MS2 in the effluent was completely removed at Fe^{3+} dosage of 0.08 mmol/L, which ensured the biosafety of drinking water. The amount of MS2 residing on the membrane's surface also dropped to 3.84 log PFU/cm^2. Viruses remaining were still infectious and would pose risks to the entire water treatment process. Therefore, chemical cleaning was implemented in the subsequent experiment to eliminate MS2 remaining on the membrane surface.

Fig. 3 (a) MS2 in effluent and on the membrane surface after different Fe^{3+} dosages treatment; (b) membrane flux after Fe^{3+} treatment; (c) membrane fouling resistance Fe^{3+} treatment; (d) UV_{254} removal by Fe^{3+} treatment.

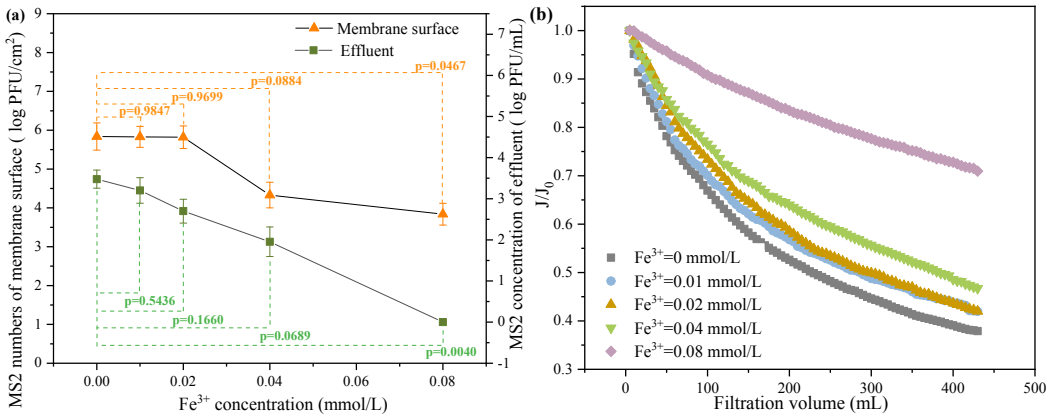

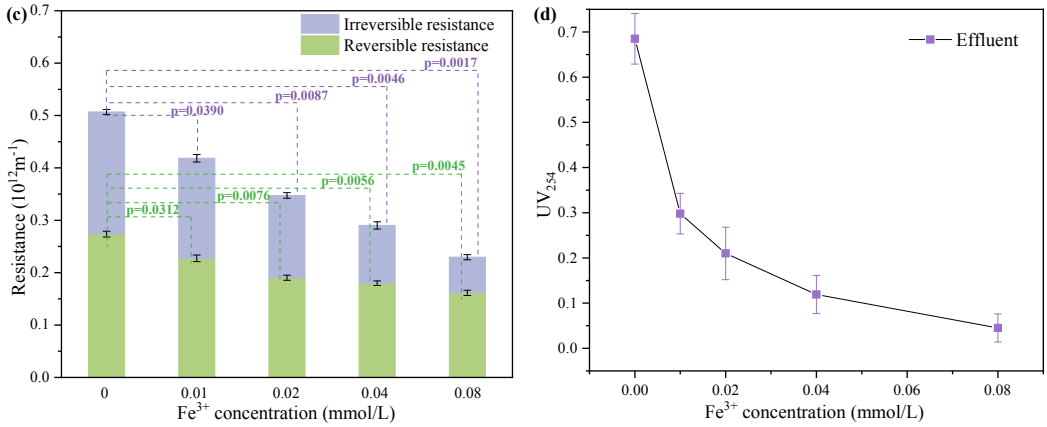

3.2.2 Performance of membrane fouling mitigation

The flux decline was effectively mitigated when the Fe^{3+} dosage increased (**Fig. 3 (b)**). The final flux rose from 0.38 to 0.71 after the pretreatment with 0.08 mmol/L Fe^{3+} and cake filtration turned into the dominant fouling mechanism with the accumulation of iron flocs (**Table 1**). This proved to be more conducive to retaining MS2.

The reversible & irreversible fouling resistances were mitigated with Fe^{3+} dosage improvement (**Fig. 3 (c)**). There was a significant change in the proportion of reversible and irreversible fouling while the total fouling resistance decreased, with a significant decline in the proportion of irreversible fouling. This would facilitate pollutant removal in the membrane cleaning process. 0.08 mmol/L Fe^{3+} decreased reversible fouling resistances to 1.62×10^{11} m^{-1} with a removal rate of 41.0%. Irreversible fouling resistance was reduced to 0.68×10^{11} m^{-1} and the removal rates reached 70.8%, which meant that Fe^{3+} treatment was more effective in irreversible fouling alleviation caused by HA and MS2. **Fig. 3 (d)** also visually proves that organics were effectively removed and the removal rate reached 93.4% at the Fe^{3+} dosage of 0.08 mmol/L. This in effect reduced the burden of subsequent UF and alleviated membrane fouling.

3.2.3 Solution characteristics changes

The solution Zeta potential got closer to 0 mV with the increase of Fe^{3+} dosage (**Fig. 4 (a)**), confirming the enhancement of coagulation performance, which was beneficial to the formation of iron flocs. Fe^{3+} with high positive charge would neutralize and adsorb negatively charged MS2 (has an isoelectric point of 3.9), and thereby promote the removal of MS2 in the solution [49]. In addition, the electrostatic interactions among MS2 and iron flocs may cause damage to the viral capsid [29, 50]. Significantly increased solution particle size (**Fig. 4 (b)**) suggested the formation of flocs and promoted coagulation performance.

3.2.4 Fe^{3+} pretreatment as a virus removal mechanism

The cake layer formed by iron flocs can retain more MS2 through size exclusion. Fe^{3+} neutralized the negative charge of the solution and membrane surface caused by HA (**Fig. 2 (a) and Fig. 4 (a)**). The interaction force between particles in the solution after Fe^{3+} treatment became an attractive force, indicating MS2 was removed by the adsorption of Fe^{3+} (**Fig. 2 (b)**) [30]. The TEM image of MS2 proved that MS2 has a distinct head-to-tail structure with a diameter of about 25 nm **(Fig. 4 (c)).** The head of MS2 has a negative charge and the tail is positively charged, making the MS2 negatively charged overall [51, 52]. The head of MS2 was adsorbed around the iron flocs and subsequently removed after Fe^{3+} pretreatment (**Fig. 4 (d)**). In addition, Fe^{3+} pretreatment enhanced electrostatic repulsion between membrane surface and the foulants (**Fig. 2 (c)**), which was beneficial to MS2 removal. Fe^{3+} treatment increased membrane surface hydrophilicity, indicating two things: firstly, viruses remaining on the membrane surface diminished; and secondly, the increase

in hydrophilicity was conducive to pollutant removal [39] **(Table 2)**.

In summary, MS2 in the solution was removed by the adsorption and size exclusion of Fe^{3+}, while the main mechanism of MS2 removal on the membrane surface was electrostatic repulsion. Although the hydrophilicity enhancement of the membrane surface was not conducive to virus removal, it is beneficial for pollutant removal and membrane fouling mitigation.

Fig. 4 (a) Zeta potential of the effluent after Fe^{3+} treatment; (b) Particle size of Fe^{3+} pretreatment and iron flocs-H_2O_2 cleaning; (c) TEM images of MS2; (d) TEM images after 0.08 mmol/L Fe^{3+} treatment; (e) TEM images after 0.08 mmol/L Fe^{3+} and 3% H_2O_2 treatment.

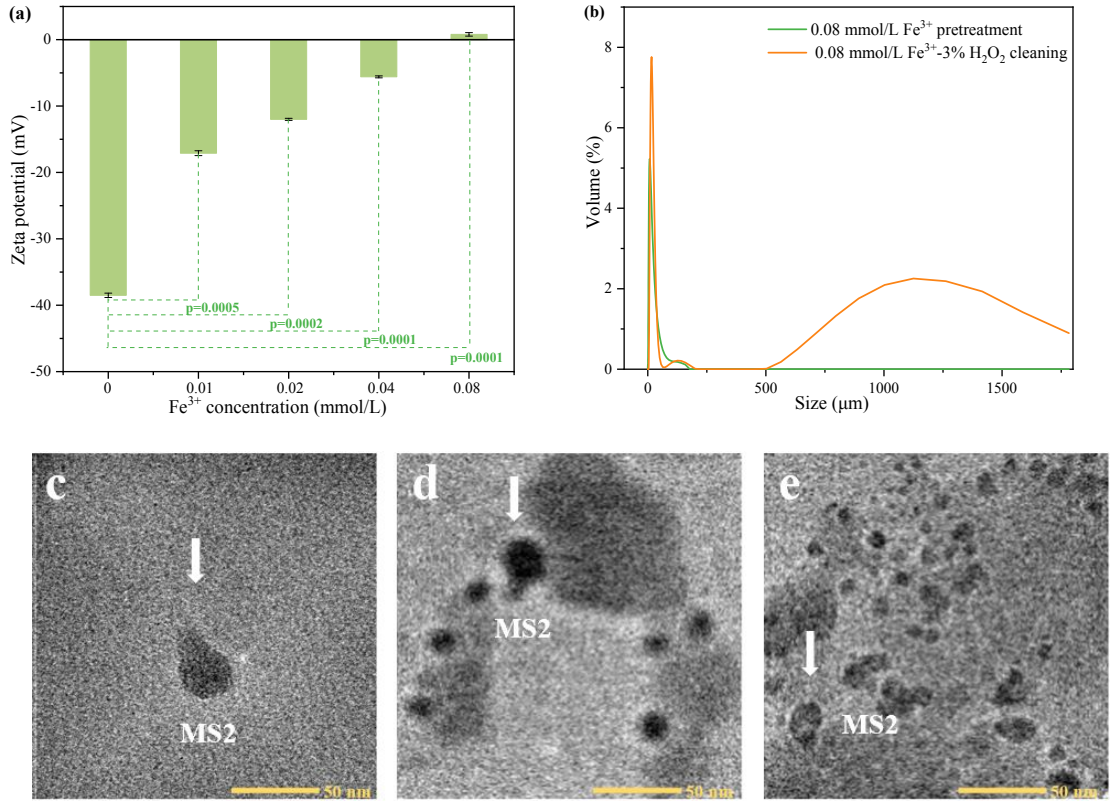

3.3 Mechanism of iron flocs-H_2O_2 in-situ cleaning on MS2 elimination and membrane fouling mitigation

3.3.1 MS2 elimination on the membrane surface

Fig. S2 reflected the residual iron on the membrane surface. There was 0.05 mg/cm^2 iron remaining on the membrane surface when Fe^{3+} dosage was 0.08 mmol/L. Iron flocs after coagulation coupled with H_2O_2 cleaning revealed significant removal of MS2 remaining on the membrane's surface (**Fig. 5 (a)**). As well, the overall cost of H_2O_2 was greatly reduced. H_2O_2 with a concentration of 12% was required to completely inactivate MS2 on the membrane surface when feedwater was not pretreated with Fe^{3+}. Compared to this, H_2O_2 with a concentration of only 3% could remove all residual MS2 under the catalysis of iron flocs.

Fig. 5 (a) Virus removal on the membrane surface after iron flocs-H_2O_2 cleaning under different concentrations; (b) Membrane fouling resistance mitigation and (c) flux recovery ratio after iron flocs-H_2O_2 cleaning.

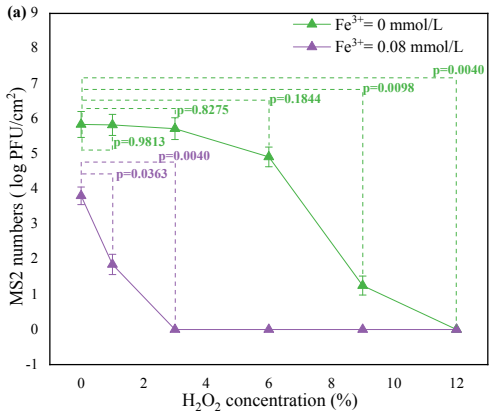

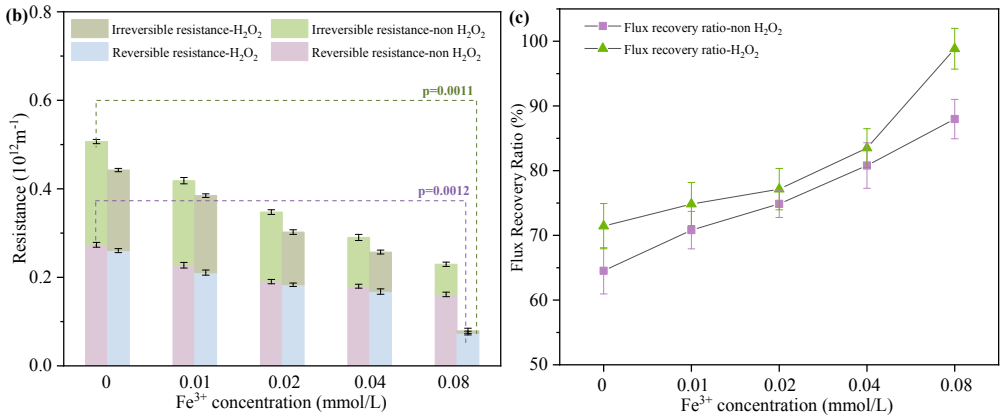

3.3.2 Membrane fouling resistance and flux recovery ratio

Fig. 5 (b) highlights membrane fouling resistance alleviation efficiency under and without 3% H_2O_2 cleaning. Compared to the non-H_2O_2 cleaning groups, both reversible and irreversible fouling resistance were significantly alleviated by iron flocs coupled with H_2O_2 cleaning. 71.5% reversible fouling resistance was mitigated, which declined from 2.60×10^{11} m^{-1} to 0.74×10^{11} m^{-1}, while irreversible resistance was more effectively mitigated from 1.82×10^{11} m^{-1} to 0.05×10^{11} m^{-1} and the removal rate reached 97.3%. As an important contributor to virus removal, irreversible fouling resistance will block membrane pores and retain more viruses [35]. The efficient removal of irreversible resistance marked high removal rates for viruses. Moreover, irreversible resistance proved to be an important factor that causes membrane aging [53], which was significantly reduced by iron flocs-H_2O_2 cleaning. The flux recovery ratio was also effectively promoted and reached 97.8% after iron flocs-H_2O_2 cleaning as displayed in **Fig. 5 (c),** which was greatly improved compared with individual Fe^{3+} pretreatment (72.9%). Reducing the amount of H_2O_2 not only saved costs but also avoid membrane damage caused by excessive membrane cleaning agent.

3.3.3 Virus elimination mechanism using iron flocs-H_2O_2 for in-situ cleaning

H_2O_2 reacted with iron flocs remaining on the membrane surface to generate HO· with strong oxidizing properties (**Fig. 6 (a)**), which could not only effectively inactivate viruses but also mitigate membrane fouling. Many studies have shown that HO· can cause higher viral deactivation rate, even in the presence of NOM [29]. TEM image demonstrates that the iron flocs had a stronger adsorption capacity for viruses after the addition of H_2O_2, and the size of flocs improved (**Fig. 4 (e)**). The electronegativity of the membrane surface was improved by iron flocs-H_2O_2 treatment (-22.51 mV), which contributed to the further removal of residual MS2 (**Fig. 2 (a)**). Iron flocs-H_2O_2 greatly promoted attractive force in the solution (**Fig. 2 (b)**), and the results of particle size and TEM image proved that flocs with larger particle size and specific surface area were formed (**Fig. 2 (c) and Fig. 4 (e)**), which could adsorb more MS2. Iron flocs-H_2O_2 cleaning formed a strong repulsive force between MS2 and the membrane surface (**Fig. 2 (c)**) and completely removed all MS2 that remained on the membrane surface. The enhancement of electrostatic interactions will cause damage to the viral capsid [50]. This surface's hydrophilicity was further enhanced by iron flocs-H_2O_2 cleaning, which contributed to the alleviation of membrane fouling and flux recovery **(Table 2)**.

Fig. 6 (a) EPR signals of Fe^{3+}-H_2O_2 reaction with DMPO as the spin trapping agent; (b) FTIR spectra of the membrane surface after different treatments; (c) FTIR spectra with a wavenumber field of 1300-1900 cm^{-1}; (d) effect of Fe^{3+} treatment and Fe^{3+}-H_2O_2 cleaning on secondary structures of the MS2 capsid protein; (e) MS2 removal mechanism in each

347 treatment stage.

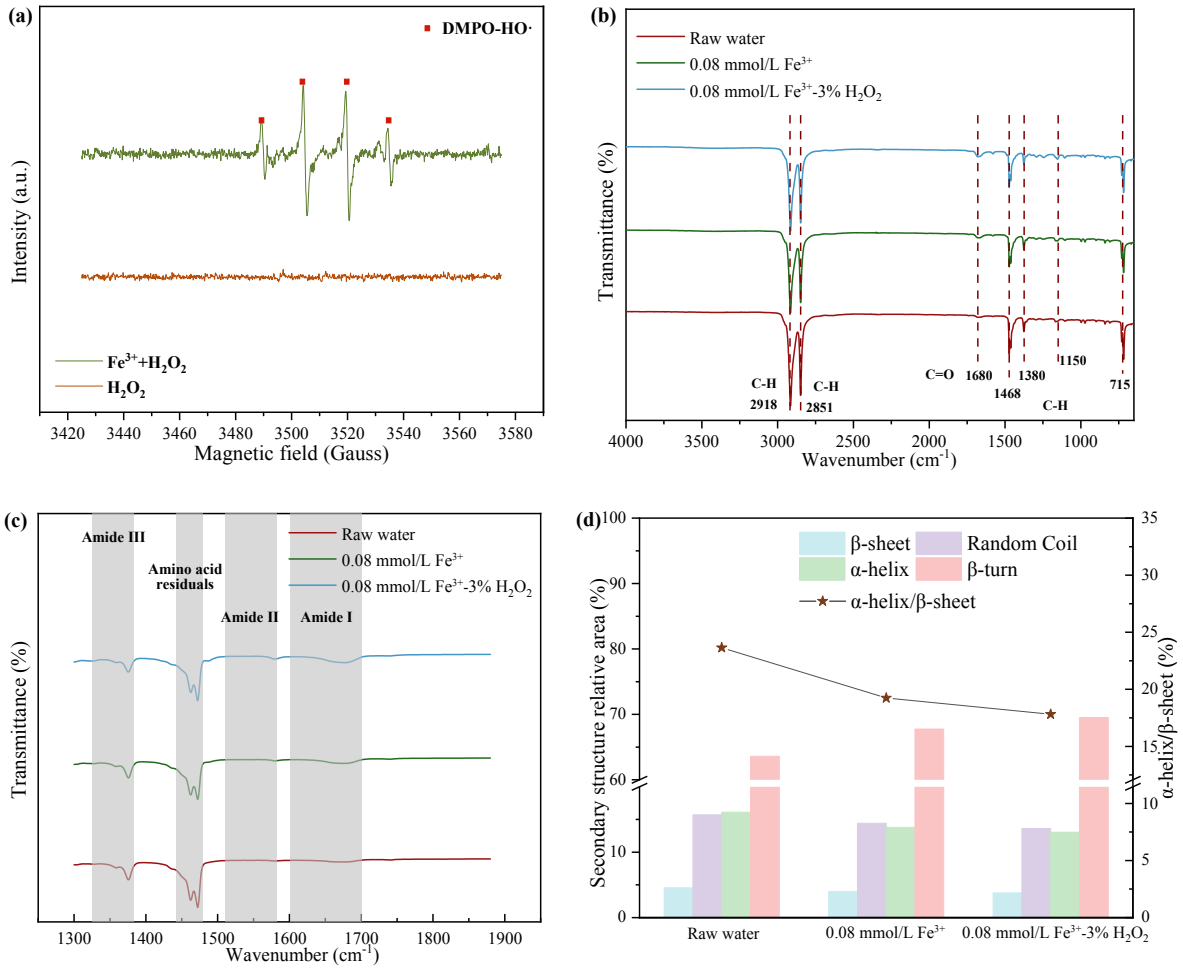

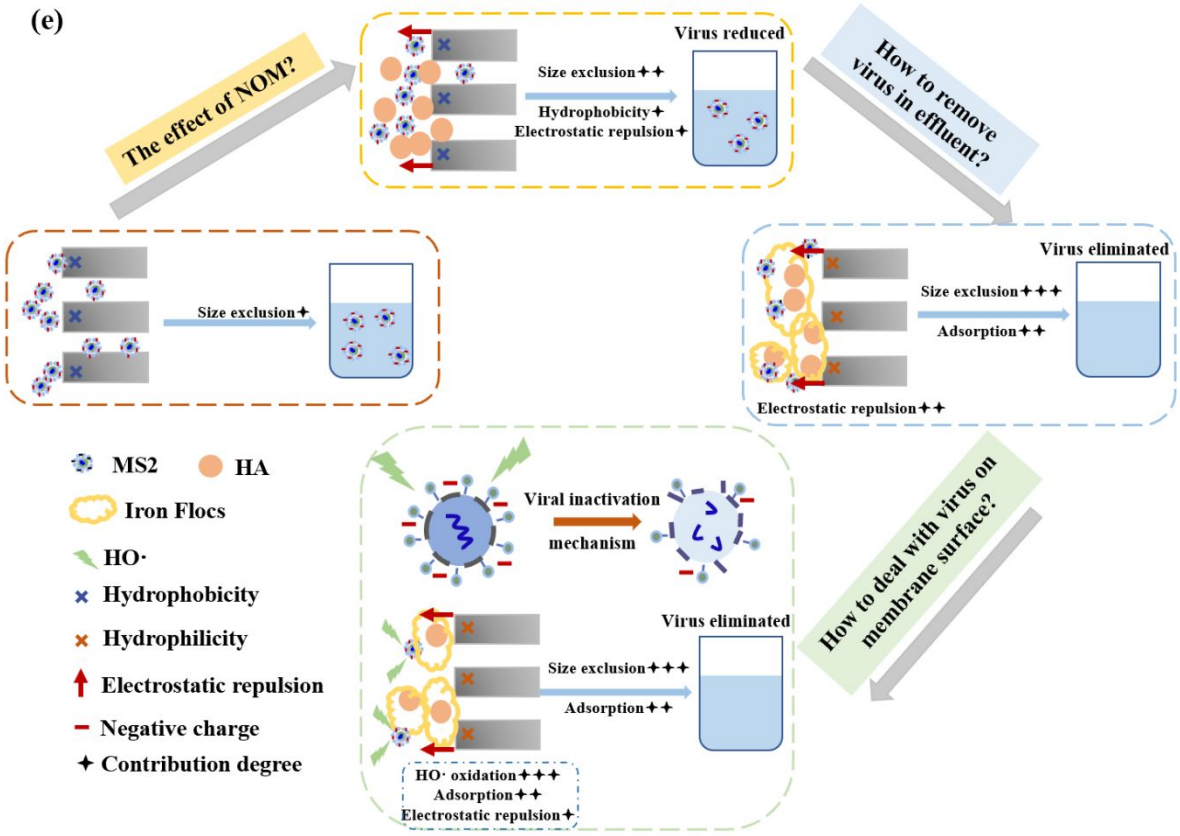

348

349 The changes of functional groups and protein structure of MS2 were analyzed by
350 FTIR. The two peaks on the left of the FTIR spectrum (2918 and 2851 cm^{-1}) represented C-
351 H stretching vibration, which was related to humic substances (**Fig. 6 (b)**). The peaks in the
352 amide I region represented C=O, which was related to the changes in protein substances
353 (**Fig. 6 (c)**). There were obvious changes in this region compared with the raw water after
354 iron flocs-H_2O_2 cleaning, indicating that the MS2 capsid protein structure and properties
355 have changed. In addition, the peaks at the amide II and III regions decreased after iron
356 flocs-H_2O_2 treatment, while the amino acid residues increased. It also proved that the
357 protein structure of the virus capsid was destroyed [54]. **Fig. 6 (d)** analyzed the transformation
358 in the secondary structure of proteins after Fe^{3+} treatment and iron flocs-H_2O_2 cleaning. α-
359 helix that could maintain the conformational stability of protein decreased after treatment

[54-56]. Moreover, the ratio decline of α-helix/β sheet suggested the formation of protein aggregates and protein acetylation. The results of FTIR demonstrated that the structure of virus capsid protein was affected by Fe^{3+} treatment and iron flocs-H_2O_2 cleaning and resulting in capsid damage, which may exacerbate viral genome release and degradation.

The mechanisms for removing MS2 under different treatment stages were summarized in **Fig. 6 (e).**

3.4 Application and prospects

During the treatment of pathogenic microorganisms-containing natural surface water by membrane technology, viruses that pass through the membrane pores and are trapped on the membrane surface will pose a hidden danger to drinking water biosafety. Therefore, effective treatment methods for removing a virus in the effluent and on the membrane surface are required. In our experiments, the viruses in the effluent can be completely removed by Fe^{3+} coagulation, and the iron flocs catalyze H_2O_2 has both disinfection and membrane cleaning functions, which will create an enhanced membrane cleaning process to improve the elimination of viruses that are retained by the membrane and mitigate membrane fouling. Iron coagulants are not only inexpensive but also 'green' and environmentally friendly, which can guarantee the biosafety of effluent and effectively alleviate membrane fouling. Furthermore, the iron flocs remaining on the membrane surface will react with H_2O_2 to generate $HO^{\cdot}$, which can further inactivate viruses and prevent membrane fouling.

Different degrees of damage to the membrane will be caused by chemical cleaning.

NaOCl is the most likely to cause membrane aging, which can lead to membrane degradation and structural damage, and even a small amount of addition will show a greater impact on the performance of UF membrane [38, 57]. The amount of H_2O_2 is greatly reduced when coupled with Fe^{3+} pretreatment, which will save membrane cleaning costs and avoid damage to the membrane caused by too much chemical cleaning agent. The results of our experiment can provide useful technical references for the treatment of virus-containing raw water in practical applications. Furthermore, the method not only can ensure the biosafety of drinking water but also reduce the usage of disinfectants after membrane treatment process, thereby curtailing the disinfection by-products (DBPs) generation. Future research on the effect of multiple coagulants and membrane cleaning agents on virus removal during membrane treatment can be undertaken, the degree of membrane damage and aging caused by chemical cleaning can also be explored, and provide more treatment methods for improving the biosafety of drinking water.

5. Conclusion

In this study, iron flocs after Fe^{3+} coagulation were used to enhance H_2O_2 cleaning for virus removal in the UF process when HA was presented. MS2 in the effluent can be eliminated by pre-coagulation. Meanwhile, the in-situ cleaning of iron flocs-H_2O_2 ensured all MS2 retained by the membrane could be inactivated. This method has practical application potential and can significantly save operating costs and extend the service life of the membrane. The mechanism for removing and inactivating the virus was also investigated. The main conclusions are as follows:

1. Virus removal in UF effluent was partly promoted through size exclusion, hydrophobicity, and electrostatic repulsion in the presence of HA. As well, HA increased the repulsion between membrane surface and MS2, slightly decreasing the residual virus found on the membrane surface.

2. Fe^{3+} coagulation reduced the burden of UF and enhanced membrane surface hydrophilicity, which effectively alleviated membrane fouling. MS2 in the effluent was completely removed by 0.08 mmol/L Fe^{3+} through adsorption and size exclusion. Any MS2 retained on the membrane surface was reduced by electrostatic repulsion.

3. Iron flocs after coagulation enhanced H_2O_2 cleaning and formed in-situ oxidation, which completely inactivated MS2 remaining on the membrane surface with low concentration H_2O_2 (3%). Membrane fouling was further alleviated and the maximum flux recovery rate reached 97.8%.

4. Iron flocs-H_2O_2 inactivated virus by generating HO· oxidation and causing virus capsid protein damage. The electrostatic repulsion and adsorption mechanism also contributed to virus removal.

Author information

Corresponding Author

An Ding - *State Key Laboratory of Urban Water Resource and Environment, School of Environment, Harbin Institute of Technology, Harbin, 150090, P. R. China;* E-mail: dinganhit@163.com

Author

Zixiao Ren - *State Key Laboratory of Urban Water Resource and Environment, School of Environment, Harbin Institute of Technology, Harbin, 150090, P. R. China*

Huicong Shi - *State Key Laboratory of Urban Water Resource and Environment, School of Environment, Harbin Institute of Technology, Harbin, 150090, P. R. China*

Jie Zeng - *State Key Laboratory of Urban Water Resource and Environment, School of Environment, Harbin Institute of Technology, Harbin, 150090, P. R. China*

Xu He - *State Key Laboratory of Urban Water Resource and Environment, School of Environment, Harbin Institute of Technology, Harbin, 150090, P. R. China*

Guibai Li - *State Key Laboratory of Urban Water Resource and Environment, School of Environment, Harbin Institute of Technology, Harbin, 150090, P. R. China*

Huu Hao Ngo - Faculty of Engineering, University of Technology Sydney, P.O. Box 123, Broadway, Sydney, NSW 2007, Australia

Jun Ma - *State Key Laboratory of Urban Water Resource and Environment, School of Environment, Harbin Institute of Technology, Harbin, 150090, P. R. China*

Chuyang Y. Tang - *Department of Civil Engineering, The University of Hong Kong, Pokfulam, Hong Kong 999077, China*

Author contributions

Zixiao Ren: Data curation, Data analyses, Writing. **Huicong Shi:** Data curation, Data analyses. **Jie Zeng:** Data curation, Data analyses. **Xu He:** Conceptualization, Methodology, Editing. **Guibai Li:** Conceptualization, Methodology, Supervision. **Huu Hao Ngo:** Conceptualization, Methodology, Editing. **Jun Ma:** Conceptualization, Methodology,

Editing. **Chuyang Y. Tang:** Revision, Editing. **An Ding:** Conceptualization, Methodology, Editing, Supervision.

Acknowledgments

The work was supported by National Natural Science Foundation of China (No. 52070058); State Key Laboratory of Urban Water Resource and Environment (Harbin Institute of Technology) (No. 2021TS17); Heilongjiang Touyan Innovation Team Program (HIT-SE-01).

References:

1. Cheng, X.; Zhang, Y.; Fan, Q.; Wang, L.; Shi, S.; Luo, X.; Zhu, X.; Wu, D.; Liang, H., Preparation of Co3O4@carbon nanotubes modified ceramic membrane for simultaneous catalytic oxidation and filtration of secondary effluent. *Chemical Engineering Journal* **2023,** *454*, 140450.

2. Ferrer, O.; Casas, S.; Galvañ, C.; Lucena, F.; Bosch, A.; Galofré, B.; Mesa, J.; Jofre, J.; Bernat, X., Direct ultrafiltration performance and membrane integrity monitoring by microbiological analysis. *Water Research* **2015,** *83*, 121-131.

3. Lian, J.; Cheng, X.; Zhu, X.; Luo, X.; Xu, J.; Tan, F.; Wu, D.; Liang, H., Mutual activation between ferrate and calcium sulfite for surface water pre-treatment and ultrafiltration membrane fouling control. *Science of The Total Environment* **2023,** *858*, 159893.

4. Ding, A.; Ren, Z.; Zhang, Y.; Ma, J.; Bai, L.; Wang, B.; Cheng, X., Evaluations of holey graphene oxide modified ultrafiltration membrane and the performance for water purification. *Chemosphere* **2021,** *285*, 131459.

5. Ren, Z.; Cheng, X.; Li, P.; Luo, C.; Tan, F.; Zhou, W.; Liu, W.; Zheng, L.; Wu, D., Ferrous-activated sodium percarbonate pre-oxidation for membrane fouling control during ultrafiltration of algae-laden water. *Science of The Total Environment* **2020,** *739*, 140030.

6. Lee, S.; Ihara, M.; Yamashita, N.; Tanaka, H., Improvement of virus removal by pilot-scale coagulation-ultrafiltration process for wastewater reclamation: Effect of optimization of pH in secondary effluent. *Water research* **2017,** *114*, 23-30.

7. Shirasaki, N.; Matsushita, T.; Matsui, Y.; Murai, K., Assessment of the efficacy of membrane filtration processes to remove human enteric viruses and the suitability of bacteriophages and a plant virus as surrogates for those viruses. *Water research* **2017,** *115*, 29-39.

8. Prevost, B.; Goulet, M.; Lucas, F.; Joyeux, M.; Moulin, L.; Wurtzer, S., Viral persistence in surface and drinking water: Suitability of PCR pre-treatment with intercalating dyes. *Water research* **2016,** *91*, 68-76.

9. Leisi, R.; Widmer, E.; Gooch, B.; Roth, N. J.; Ros, C., Mechanistic insights into flow-dependent virus retention in different nanofilter membranes. *Journal of Membrane Science* **2021,** *636*, 119548.

10. Al-Hazmi, H. E.; Shokrani, H.; Shokrani, A.; Jabbour, K.; Abida, O.; Mousavi Khadem, S. S.; Habibzadeh, S.; Sonawane, S. H.; Saeb, M. R.; Bonilla-Petriciolet, A.; Badawi, M., Recent advances in aqueous virus removal technologies. *Chemosphere* **2022,** *305*, 135441.

11. Symonds, E. M.; Verbyla, M. E.; Lukasik, J. O.; Kafle, R. C.; Breitbart, M.; Mihelcic, J. R., A case study of enteric virus removal and insights into the associated risk of water reuse for two wastewater treatment pond systems in Bolivia. *Water Research* **2014,** *65*, 257-270.

12. Goswami, K. P.; Pugazhenthi, G., Credibility of polymeric and ceramic membrane filtration in the removal of bacteria and virus from water: A review. *Journal of Environmental Management* **2020,** *268*, 110583.

13. Domagała, K.; Jacquin, C.; Borlaf, M.; Sinnet, B.; Julian, T.; Kata, D.; Graule, T., Efficiency and stability evaluation of Cu2O/MWCNTs filters for virus removal from water. *Water Research* **2020,** *179*, 115879.

14. Kreißel, K.; Bösl, M.; Lipp, P.; Franzreb, M.; Hambsch, B., Study on the removal efficiency of UF membranes using bacteriophages in bench-scale and semi-technical scale. *Water Science and Technology* **2012,** *66*, (6), 1195-1202.

15. Zhu, Y.; Chen, R.; Li, Y.-Y.; Sano, D., Virus removal by membrane bioreactors: A review of mechanism investigation and modeling efforts. *Water Research* **2021,** *188*, 116522.

16. Palika, A.; Armanious, A.; Rahimi, A.; Medaglia, C.; Gasbarri, M.; Handschin, S.; Rossi, A.; Pohl, M. O.; Busnadiego, I.; Gübeli, C., An antiviral trap made of protein nanofibrils and iron oxyhydroxide nanoparticles. *Nature Nanotechnology* **2021,** *16*, (8), 918-925.

17. Shen, M.-H.; Yin, Y.-G.; Booth, A.; Liu, J.-F., Effects of molecular weight-dependent physicochemical heterogeneity of natural organic matter on the aggregation of fullerene nanoparticles in mono-and di-valent electrolyte solutions. *Water Research* **2015,** *71*, 11-20.

18. Szermer-Olearnik, B.; Drab, M.; Mąkosa, M.; Zembala, M.; Barbasz, J.; Dąbrowska, K.; Boratyński, J., Aggregation/dispersion transitions of T4 phage triggered by environmental ion availability. *Journal of nanobiotechnology* **2017,** *15*, (1), 1-15.

19. ElHadidy, A. M.; Peldszus, S.; Van Dyke, M. I., Effect of hydraulically reversible

and hydraulically irreversible fouling on the removal of MS2 and φX174 bacteriophage by an ultrafiltration membrane. *Water Research* **2014,** *61*, 297-307.

20. Ren, Z.; Cao, H.; Desmond, P.; Liu, B.; Ngo, H. H.; He, X.; Li, G.; Ma, J.; Ding, A., Ions play different roles in virus removal caused by different NOMs in UF process: Removal efficiency and mechanism analysis. *Chemosphere* **2023,** *313*, 137644.

21. Kloster, N.; Brigante, M.; Zanini, G.; Avena, M., Aggregation kinetics of humic acids in the presence of calcium ions. *Colloids and Surfaces A: Physicochemical and Engineering Aspects* **2013,** *427*, 76-82.

22. Bai, Z.; Gao, S.; Yu, H.; Liu, X.; Tian, J., Layered metal oxides loaded ceramic membrane activating peroxymonosulfate for mitigation of NOM membrane fouling. *Water Research* **2022,** *222*, 118928.

23. Zhu, B.; Clifford, D. A.; Chellam, S., Comparison of electrocoagulation and chemical coagulation pretreatment for enhanced virus removal using microfiltration membranes. *Water Research* **2005,** *39*, (13), 3098-3108.

24. Ding, A.; Ren, Z.; Hu, L.; Zhang, R.; Ngo, H. H.; Lv, D.; Nan, J.; Li, G.; Ma, J., Oxidation and coagulation/adsorption dual effects of ferrate (VI) pretreatment on organics removal and membrane fouling alleviation in UF process during secondary effluent treatment. *Science of The Total Environment* **2022,** *850*, 157986.

25. Chen, M.; Nan, J.; Ji, X.; Wu, F.; Ye, X.; Ge, Z., Effect of adsorption and coagulation pretreatment sequence on ultrafiltration membrane fouling: Process study and targeted prediction. *Desalination* **2022,** *540*, 115967.

26. Gan, Y.; Zhang, L.; Zhang, S., The suitability of titanium salts in coagulation removal of micropollutants and in alleviation of membrane fouling. *Water Research* **2021,** *205*, 117692.

27. Kreißel, K.; Bösl, M.; Hügler, M.; Lipp, P.; Franzreb, M.; Hambsch, B., Inactivation of F-specific bacteriophages during flocculation with polyaluminum chloride–a mechanistic study. *Water Research* **2014,** *51*, 144-151.

28. Zhu, B.; Clifford, D. A.; Chellam, S., Virus removal by iron coagulation–microfiltration. *Water Research* **2005,** *39*, (20), 5153-5161.

29. Giannakis, S.; Liu, S.; Carratalà, A.; Rtimi, S.; Talebi Amiri, M.; Bensimon, M.; Pulgarin, C., Iron oxide-mediated semiconductor photocatalysis vs. heterogeneous photo-Fenton treatment of viruses in wastewater. Impact of the oxide particle size. *Journal of Hazardous Materials* **2017,** *339*, 223-231.

30. Tanneru, C. T.; Chellam, S., Mechanisms of virus control during iron electrocoagulation–Microfiltration of surface water. *Water research* **2012,** *46*, (7), 2111-2120.

31. Gan, X.; Lin, T.; Jiang, F.; Zhang, X., Impacts on characteristics and effluent safety of PVDF ultrafiltration membranes aged by different chemical cleaning types. *Journal of Membrane Science* **2021,** *640*, 119770.

32. He, X.; Li, B.; Wang, P.; Ma, J., Novel H2O2–MnO2 system for efficient physico-chemical cleaning of fouled ultrafiltration membranes by simultaneous generation of reactive free radicals and oxygen. *Water Research* **2019,** *167*, 115111.

33. Bao, X.; Liu, Q.; Yang, J.; Wang, F.; Yu, F.; Yu, J.; Yang, Y., Cascading in-situ generation of H2O2 and Fenton-like reaction in photocatalytic composite ultrafiltration membrane for high self-cleaning performance in wastewater treatment. *Journal of Membrane Science* **2022,** *660*, 120866.

34. Tobias, A.; Bérubé, P. R., Contribution of biofilm layer to virus removal in gravity-driven membrane systems with passive fouling control. *Separation and Purification Technology* **2020,** *251*, 117336.

35. Marti, E.; Monclús, H.; Jofre, J.; Rodriguez-Roda, I.; Comas, J.; Balcázar, J. L., Removal of microbial indicators from municipal wastewater by a membrane bioreactor (MBR). *Bioresource Technology* **2011,** *102*, (8), 5004-5009.

36. ElHadidy, A. M.; Peldszus, S.; Van Dyke, M. I., An evaluation of virus removal mechanisms by ultrafiltration membranes using MS2 and φX174 bacteriophage. *Separation and Purification Technology* **2013,** *120*, 215-223.

37. Cai, W.; Liu, Y., Comparative study of dissolved organic matter generated from activated sludge during exposure to hypochlorite, hydrogen peroxide, acid and alkaline: Implications for on-line chemical cleaning of MBR. *Chemosphere* **2018,** *193*, 295-303.

38. Regula, C.; Carretier, E.; Wyart, Y.; Gésan-Guiziou, G.; Vincent, A.; Boudot, D.; Moulin, P., Chemical cleaning/disinfection and ageing of organic UF membranes: A review. *Water Research* **2014,** *56*, 325-365.

39. Li, B.; Ma, J.; Qiu, W.; Li, W.; Zhang, B.; Ding, A.; He, X., In-situ utilization of membrane foulants (FeOx+MnOx) for the efficient membrane cleaning. *Water Research*

2022, *210*, 118004.

40. Mamane, H.; Shemer, H.; Linden, K. G., Inactivation of E. coli, B. subtilis spores, and MS2, T4, and T7 phage using UV/H2O2 advanced oxidation. *Journal of hazardous materials* **2007,** *146*, (3), 479-486.

41. Gutierrez, L.; Li, X.; Wang, J.; Nangmenyi, G.; Economy, J.; Kuhlenschmidt, T. B.; Kuhlenschmidt, M. S.; Nguyen, T. H., Adsorption of rotavirus and bacteriophage MS2 using glass fiber coated with hematite nanoparticles. *Water Research* **2009,** *43*, (20), 5198-5208.

42. Anderson, W. B.; DeLoyde, J. L.; Van Dyke, M. I.; Huck, P. M., Influence of design and operating conditions on the removal of MS2 bacteriophage by pilot-scale multistage slow sand filtration. *Journal of Water Supply: Research and Technology—AQUA* **2009,** *58*, (7), 450-462.

43. Gentile, G. J.; Cruz, M. C.; Rajal, V. B.; de Cortalezzi, M. M. F., Electrostatic interactions in virus removal by ultrafiltration membranes. *Journal of environmental chemical engineering* **2018,** *6*, (1), 1314-1321.

44. Zheng, X.; Liu, J., Virus rejection with two model human enteric viruses in membrane bioreactor system. *Science in China Series B: Chemistry* **2007,** *50*, (3), 397-404.

45. Xiang, Z.; Wenzhou, L.; Min, Y.; Junxin, L., Evaluation of virus removal in MBR using coliphages T4. *Chinese Science Bulletin* **2005,** *50*, (9), 862-867.

46. Yin, Z.; Tarabara, V. V.; Xagoraraki, I., Human adenovirus removal by hollow fiber membranes: Effect of membrane fouling by suspended and dissolved matter. *Journal*

of Membrane Science **2015,** *482*, 120-127.

47. Wu, B.; Liu, H.; Liu, Z.; Zhang, J.; Zhai, X.; Zhu, Y.; Sano, D.; Wang, X.; Chen, R., Interface behavior and removal mechanisms of human pathogenic viruses in anaerobic membrane bioreactor (AnMBR). *Water Research* **2022,** *219*, 118596.

48. Li, X.; Cai, M.; Wang, L.; Niu, F.; Yang, D.; Zhang, G., Evaluation survey of microbial disinfection methods in UV-LED water treatment systems. *Science of the Total Environment* **2019,** *659*, 1415-1427.

49. Park, J. A.; Kim, S. B.; Lee, C. G.; Lee, S. H.; Choi, J. W., Adsorption of bacteriophage MS2 to magnetic iron oxide nanoparticles in aqueous solutions. *Environmental Letters* **2014,** *49*, (9-10), 1116-1124.

50. Mayer, B. K.; Yang, Y.; Gerrity, D. W.; Abbaszadegan, M., The Impact of Capsid Proteins on Virus Removal and Inactivation During Water Treatment Processes. *Microbiology Insights* **2015,** *8*, (Suppl 2), 15.

51. Armanious, A.; Aeppli, M.; Jacak, R.; Refardt, D.; Sigstam, T.; Kohn, T.; Sander, M., Viruses at solid–water interfaces: a systematic assessment of interactions driving adsorption. *Environmental science & technology* **2016,** *50*, (2), 732-743.

52. Michen, B.; Graule, T., Isoelectric points of viruses. *Journal of applied microbiology* **2010,** *109*, (2), 388-397.

53. Antony, A.; Branch, A.; Leslie, G.; Le-Clech, P., Impact of membrane ageing on reverse osmosis performance – Implications on validation protocol. *Journal of Membrane Science* **2016,** *520*, 37-44.

54. Yang, H.; Min, X.; Wu, J.; Lin, X.; Gao, F.-Z.; Hu, L.-X.; Zhang, L.; Wang, Y.; Xu, S.; Ying, G.-G., Removal and Inactivation of Virus by Ceramic Water Filters Coated with Lanthanum (III). *ACS ES&T Water* **2022,** *2*, (10), 1811-1821.

55. Barraza-Garza, G.; Castillo-Michel, H.; de la Rosa, L. A.; Martinez-Martinez, A.; Pérez-León, J. A.; Cotte, M.; Alvarez-Parrilla, E., Infrared spectroscopy as a tool to study the antioxidant activity of polyphenolic compounds in isolated rat enterocytes. *Oxidative Medicine and Cellular Longevity* **2016,** *2016*.

56. Hu, L.-X.; Xiong, Q.; Shi, W.-J.; Huang, G.-Y.; Liu, Y.-S.; Ying, G.-G., New insight into the negative impact of imidazolium-based ionic liquid [C10mim] Cl on Hela cells: From membrane damage to biochemical alterations. *Ecotoxicology and Environmental Safety* **2021,** *208*, 111629.

57. Gitis, V.; Haught, R. C.; Clark, R. M.; Gun, J.; Lev, O., Application of nanoscale probes for the evaluation of the integrity of ultrafiltration membranes. *Journal of Membrane Science* **2006,** *276*, (1), 185-192.